Published in final edited form as:
J Am Chem Soc. 2009 August 12; 131(31): 11041–11048. doi:10.1021/ja903038d.

Towards an Artificial Golgi: Redesigning the Biological Activities of Heparan Sulfate on a Digital Microfluidic Chip

Jeffrey G. Martin[1,2], **Megha Gupta**[3], **Yongmei Xu**[4], **Srinivas Akella**[4], **Jian Liu**[4], **Jonathan S. Dordick**[2,5], and **Robert J. Linhardt**[*,1,2,5]

[1]Department of Chemistry and Chemical Biology, Rensselaer Polytechnic Institute, Troy, New York 12180

[2]Department of Biology, Rensselaer Polytechnic Institute, Troy, New York 12180

[3]Department of Computer Science, Rensselaer Polytechnic Institute, Troy, New York 12180

[4]Division of Medicinal Chemistry and Natural Products, UNC Eshelman School of Pharmacy, University of North Carolina, Chapel Hill, NC 27599

[5]Department of Chemical and Biological Engineering, Rensselaer Polytechnic Institute, Troy, New York 12180

Abstract

Using digital microfluidics, recombinant enzyme technology, and magnetic nanoparticles, we have created a functional prototype of an artificial Golgi organelle. Analogous to the natural Golgi, which is responsible for the enzymatic modification of glycosaminoglycans immobilized on proteins, this artificial Golgi enzymatically modifies glycosaminoglycans, specifically heparin sulfate (HS) chains immobilized onto magnetic nanoparticles. Sulfo groups were transferred from adenosine 3′-phosphate 5′-phosphosulfate to the 3-hydroxyl group of the D-glucosamine residue in an immobilized HS chain using D-glucosaminyl 3-*O*-sulfotransferase. After modification, the nanoparticles with immobilized HS exhibited increased affinity for fluorescently labeled antithrombin III as detected by confocal microscopy. Since the biosynthesis of HS involves an array of specialized glycosyl transferases, epimerase, and sulfotransferases, this approach should mimic the synthesis of HS *in vivo*. Furthermore, our method demonstrates the feasibility of investigating the effects of multi-enzyme systems on the structure of final glycan products for HS-based glycomic studies.

Introduction

The Golgi organelle, discovered in 1898 by Camillo Golgi, remains one of the most poorly understood organelles in the human cell. This organelle is central to the posttranslational modification of proteins, the new frontier in the field of glycomics. It is estimated that the majority of human proteins are posttranslationally modified within the Golgi,[1] primarily through glycosylation, and that these modifications are critical for protein function and stability.

Heparan sulfate (HS) glycosylation of proteoglycans (PGs) takes place in the Golgi organelle (Figure 1a). Linear, *O*-linked glycosaminoglycan (GAG) chains composed of repeating glucuronic acid and *N*-acetylglucosamine residues are attached to the serine residues of a core

*linhar@rpi.edu.

Supporting Information Available: Time course data, additional confocal images used for statistical analysis, and the complete reference 15 are provided as a PDF. This information is available free of charge via the Internet at http://pubs.acs.org.

protein through a linkage region to form a PG and are sequentially modified by a series of biosynthetic enzymes including an *N*-deacetylase/*N*-sulfotransferase (NDST), C_5 epimerase, and 2-, 6-, and 3-*O*-sulfotransferases (2-OST, 6-OST and 3-OST, respectively). NDST catalyzes the *N*-deacetylation/*N*-sulfonation of the glucosamine residues, C_5 epimerase converts glucuronic acid into iduronic acid, and 2-OST, 6-OST, and 3-OST catalyze the *O*-sulfonation of the 2-*O*-position of the uronic acid, and the 6-*O* and 3-*O*-positions of the glucosamine unit, respectively.[2,3] There is also an alternative theory of GAG biosynthesis that suggests the concerted action between one or more of the biosynthetic enzymes.[4]

Many of these modifications in the Golgi are only partially complete, resulting in a large number of sequence permutations, dramatically complicating the structure of HS.[4] The ensemble of the GAG chains afforded contain different and often unique structural features that determine their protein binding specificity and ultimate biological activity. PGs synthesized with specific GAG chains are found in the extracellular matrix, and on the surface of mammalian cells. They are involved in important physiological and pathophysiological processes including blood coagulation, infection, cellular growth and differentiation, tumor metastasis, and angiogenesis.[5]

It is believed that the structure of the Golgi apparatus contributes to the structure of HS. Unfortunately, the complexity of the Golgi apparatus limits our understanding of HS biosynthesis. Because studying the *in vitro* enzymatic synthesis of HS in the absence of a Golgi structure cannot permit a full understanding of the control and regulation of HS biosynthesis, we undertook the design and fabrication of an artificial Golgi using a digital microfluidic platform (Figure 1b) that resembles the natural organelle. This work represents the first step toward the creation of such a biomimetic organelle.

Microfluidics and lab-on-a-chip technologies enable reactions on the micro- and nanoscales, reducing reagent consumption and analysis time, increasing reaction control and throughput, and providing opportunities for full automation.[6] Two types of microfluidic systems have been developed: 1) channel microfluidics, which involves fluid flow in patterned channels,; and 2) digital microfluidics, wherein open droplet movement occurs through the process of electrowetting on a 2D grid-like platform. Digital microfluidics has gained popularity by eliminating many of the constraints associated with fixed channels[7] and allowing individual droplets in a biochemical array to be addressed. Some previous applications of digital microfluidics include glucose and other enzyme-based assays, preparation of protein samples for matrix-assisted laser desorption/ionization mass spectrometry, polymerase chain reaction, and cell-based assays.[8]

Digital microfluidics chips consist of an array of electrodes (Figure 1c) coated with an insulator followed by a hydrophobic layer (Figure 1d). Droplet movement in digital microfluidics is driven by electrowetting, the ability of a surface to tune its wettability by the application of electrical pulses. To operate a digital microfluidic device, a droplet of fluid is placed over one electrode and then a voltage is applied to an adjacent electrode, causing the insulator above that electrode to become charged. This makes the destination electrode more hydrophilic causing the droplet to move.[9] This wettablity of the surface is reversible, thus allowing the droplet to be moved to an adjacent electrode of choice. In this manner, sample-containing droplets may be transported, mixed, and separated on the chip.

The current study investigates the modification of HS by D-glucosaminyl 3-*O*-sulfotransferase isoform-1 (3-OST-1) using digital microfluidics to afford an HS with an increased affinity for anticoagulant protein antithrombin III (ATIII). This represents a first step towards the construction of an artificial Golgi organelle that may serve as a test-bed to better understand how the natural Golgi controls the biosynthesis of GAGs.

Experimental Section

Chip fabrication

Microfluidic chips were fabricated using standard clean room processes at Rensselaer's Center for Integrated Electronics Micro and Nano Fabrication Clean Room using a modified clean room process from Wheeler et al.[10] Briefly, chips were designed using Macromedia Freehand (San Jose, CA) with standard dimensions of: electrode size (1 mm × 1 mm), reservoir size (3 mm × 3 mm), and electrode spacing (5 μm). Photomask transparencies constructed from these designs were made by M & J Prepress (Albany, NY). Glass slides (Thermo Fisher Scientific, Waltham, MA) were cleaned with piranha solution (7:3 concentrated sulfuric acid/30% hydrogen peroxide, 10 min), followed by coating with 10 nm of chromium (International Advanced Materials, Spring Valley, NY), and 100 nm of gold (International Advanced Materials Spring Valley, NY) by electron beam deposition. The slides were then rinsed with acetone, methanol, and DI water and baked on a hotplate at 115°C for 5 min. Substrates were spin coated with photoresist and exposed through a photomask using a Karl Suss mask aligner (Garching, Germany). The exposed substrates were developed in AZ300MIF (AZ Electronic Materials, Branchburg, NJ) for 3 min and post-baked on a hotplate. The remaining unexposed gold and chromium was then etched away. The remaining photoresist was stripped in AZ300T (AZ Electronic Materials, Branchburg, NJ) for 5 min in an ultrasonic bath. The chips were then coated with 2 μm parylene C followed by spin-coating with a 1% Teflon AF solution in FC-40 (DuPont, Wilmington, DE) at 2000 rpm for 1 min. The extra solvent was then evaporated by placing the chip on a hotplate at 160°C for 10 min. Indium-tin-oxide coated glass slides (Delta Technologies, Stillwater, MN) were also coated with a 1% Teflon AF solution and used as coverslips.

Chip operation

Electrical equipment used for chip operation included an Agilent 33220A 20 MHz Function/Arbitrary Waveform Generator (Santa Clara, CA) and a Trek Model PZD700 Dual Channel Amplifier (Medina, NY). Four basic droplet operations for digital microfluidic devices were used in this study: 1) droplet actuation; 2) dispensing; 3) splitting; and 4) mixing. Droplet actuation was achieved by applying an AC voltage 50 – 100 V_{RMS} to a destination electrode adjacent to the droplet. Sample droplets were dispensed from reservoir droplets by applying voltage to electrodes adjacent to the reservoir to draw a portion of the droplet away from the reservoir while holding the remaining bulk of the droplet within the reservoir using a separate application of voltage. After a distance of about two electrodes, surface tension caused splitting of the sample droplet from the reservoir droplet. Droplets were split by application of voltage to the electrodes adjacent to the ends of the droplet and maintaining the voltage until the splitting occurred. Droplets were mixed by actuating two droplets to the same electrode then homogenized by pulsing voltage to the electrodes adjacent to the ends of the droplet to cause stretching.

Immobilization of heparan sulfate onto magnetic nanoparticles

Sodium HS from porcine intestinal mucosa was obtained from Celsius Laboratories (Cincinnati, OH). The HS was first completely *N*-acetylated at 25°C by dissolving 200 mg of HS in 10 mL 0.05 M sodium carbonate (Sigma-Aldrich, St. Louis, MO) containing 10% methanol (Sigma-Aldrich, St. Louis, MO) and adding 80 μL acetic anhydride (Sigma-Aldrich) dropwise over a period of 2 h. The solution containing *N*-acetylated HS was then diluted with two volumes of distilled water, dialyzed (2,000 molecular weight cut-off (MWCO)) for 48 h and lyophilized. This fully *N*-acetylated heparin (100 mg) was dissolved in formamide (8.3 μM) (Sigma-Aldrich) at 50°C, 2,6-diaminopyridine (100 mg) (Sigma-Aldrich) was added, and the reaction mixture was maintained at 50°C for 3 h. Sodium cyanoborohydride (19 mg) (Sigma-Aldrich) was added and the mixture was maintained at 50°C for 24 h, diluted with 20

mL of water, dialyzed (2,000 MWCO) exhaustively for 48 h, and lyophilized. The lyophilized diaminopyridylinylated HS was further purified by SAX chromatography followed by methanol precipitation.[11] The resulting 2,6-diaminopyridinyl heparin was dissolved in phosphate buffered saline (PBS, pH 7.4) and a 20-fold molar excess of Sulfo-NHS-PEG-Biotin (5000 MW) (Nanocs, New York, NY) was added. The reaction mixture was incubated at 25° C for 1 h and then dialyzed (3,000 MWCO) to remove excess biotin. The retentate containing biotinylated HS was then lyophilized.

Using a magnetic rack (New England Biolabs, Ipswitch, MA), streptavidin magnetic nanoparticles (600 nm diameter) from MagnaMedics Diagnostics (Maastricht, The Netherlands) were washed with 0.05% Triton X-100 (Sigma-Aldrich) in PBS. Biotiylated HS was added (3-fold molar excess) to the solution of streptavidin magnetic nanoparticles and the mixture was incubated on a roller mixer at 25°C for 45 min. The nanoparticles were then washed extensively with 0.05% Triton X-100 in PBS to remove the excess biotinylated HS. The nanoparticles were further washed with PBS buffer to remove the Triton X-100 surfactant. The overall immobilization scheme is shown in Figure 2.

Quantification of heparan sulfate on magnetic nanoparticles by enzymatic digestion

HS-nanoparticles (1 mg) were incubated with 25 milliunits each of a mixture of heparin lyase 1, 2, and 3 for 24 h at 37°C to quantify the amount of HS that had been immobilized. After 24 h, the nanoparticles were isolated using the magnetic rack and the supernatant was recovered by decanting. The supernatant, containing heparin lyases and HS disaccharides, was passed through a 3,000 MWCO spin column (PALL, East Hills, NY) to recover the free HS disaccharides from the enzymes. A microscale carbazole assay was used to determine the amount of free disaccharides present from which the amount of enzyme accessible immobilized HS chains could be calculated.

Quantification of modification of heparan sulfate on nanoparticles by 3-OST

Recombinant 3-OST-1 enzyme was prepared as previously described[12] and adenosine 3′-phosphate 5′-phosphosulfate (PAPS) was obtained from Sigma-Aldrich (St. Louis, MO). [^{35}S]PAPS was prepared from ATP and sodium [^{35}S] sulfate in the presence of yeast extract (from Sigma-Aldrich).[13] Immobilized HS (about 20 μg) was incubated with purified 3-OST-1 (300 μg) and PAPS (100 μM) in 300 μL of reaction buffer containing 50 mM MES (pH 7.0), 1 mM $MgCl_2$, and 2 mM $MnCl_2$. The reaction was shaken at 30 °C at 200 RPM for 2 h. The nanoparticles were then washed with 3 × 1 mL of 250 mM NaCl followed by 3 × 1 mL of 1 M NaCl. An identical reaction was carried out by replacing unlabeled PAPS with ^{35}S-labeled PAPS to estimate the degree of 3-*O*-sulfonation. The degree of 3-*O*-sulfonation was estimated by measuring ^{35}S-radioactivity on the nanoparticles. A time course reaction was carried out by incubating immobilized HS (50 μg) with purified 3-OST-1 (100 μg) and [^{35}S]PAPS at 30 °C. The reaction was stopped periodically and an aliquot was removed, and the beads were washed with buffer containing 3 M urea followed by buffer with 1 M NaCl. The washed beads were then mixed with scintillation fluid to determine the level of incorporation of ^{35}S-label.

Synthesis of Fluorescently labeled ATIII

Amine reactive 4,4-Difluoro-5-phenyl-4-bora-3,4a-diaza-s-indacene-3-propionic acid, succinimidyl ester (BODIPY® R6G, SE) was obtained from Invitrogen Corporation (Carlsbad, CA). ATIII was obtained from Aniara (Mason, OH). BODIPY® R6G dye was covalently attached to ATIII. ATIII (10 mg) was dissolved in 1 mL of 0.1 M sodium bicarbonate buffer and BODIPY® R6G (5 mg) was dissolved in 0.5 mL anhydrous DMF (Sigma-Aldrich, St. Louis, MO). BODIPY® R6G (100 μL) was added with stirring to the ATIII solution. The reaction mixture was incubated for 1 h at room temperature with continuous stirring. After the

completion of the reaction, a 3,000 MWCO spin column was used to remove excess BODIPY® R6G. The purified BODIPY® R6G labeled ATIII was then stored at −20°C.

Off-chip enzymatic modification

PAPS and 3-OST-1 were mixed with nanoparticles in PBS then washed with distilled water as described above. The 3-OST-1 modified nanoparticles (100 μg) were incubated at 25 °C with BODIPY® R6G labeled ATIII (1 μg) in 10 mL of 2.5-fold concentrated PBS containing 0.025% Tween X-100 for 30 min. After incubation, the nanoparticles were washed with 0.05% Tween X-100 in 5-fold concentrated PBS then distilled water. The nanoparticles were imaged using a Zeiss LSM 510 META confocal microscope with a 100X/1.45 oil objective (Zeiss, Jena, Germany). A 514 nm argon laser was used to excite BODIPY® R6G and a 530 nm – 600 nm emission filter was used. A range check pseudocolored map was used to optimize the dynamic range for the images.

On-chip enzymatic modification

Two droplets, one containing 400 nL of 3-OST-1 (0.1 mg/mL) and PAPS (25 μM) in PBS and the second containing nanoparticle-immobilized HS (5 mg/mL) in PBS, were loaded onto a digital microfluidics chip into a layer of 1.0 cSt silicone oil (Gelest, Morrisville, PA) containing 0.1% Triton® X-15 (Sigma-Aldrich, St. Louis, MO). The use of silicon oil and the short duration of electrode activation reduced non-specific adsorption of protein to the surface and droplet heating. The chip was used to drive the droplets to the mixing area and perform the mixing operation by first joining the two droplets then stretching the droplet to homogenize the reaction mixture. Following the mixing operation, the reaction droplet was incubated at room temperature for 1 h with an additional homogenizing step at 30 min. Based on the results of the 3-OST-1 time course experiment (see Supporting Information Figure S1), an on-chip incubation time of 1 h was selected to allow for at least one 3-*O*-sulfonation site per HS chain, as is present in the natural polysaccharide. After the incubation was complete, the droplet was recovered using a micropipette added to an 800 nL droplet of water following addition of a 400 nL droplet containing fluorescent ATIII (0.175 mg/mL) and 0.0375% Tween 100 in 3.75-fold concentrated PBS. The 3-OST-1 modified HS-nanoparticles were incubated with fluorescent ATIII at room temperature for 30 min. After incubation, the nanoparticles were washed with 0.05% Tween X-100 in 5-fold concentrated PBS then distilled water. The nanoparticles were imaged using a Zeiss LSM 510 META confocal microscope with a 100X/1.45 oil objective (Zeiss, Jena, Germany). A 514 nm argon laser was used to excite BODIPY® R6G and a 530 nm – 600 nm emission filter was used. A range check pseudocolored map was used to optimize the dynamic range for the images. Control experiments were also conducted using a 400 nL droplet of PBS in place of the 3-OST-1 enzyme in PBS.

Analysis of confocal images

Transmitted bright field images acquired from confocal microscopy were imported in to Adobe Photoshop (Adobe Systems Incorporated, San Jose, CA) where the background was selected and filled with white. The images were then imported into ImageJ (National Institutes of Health, Bethesda, MD) and converted to 16-bit grayscale. The ImageJ analyze particle feature was used to determine the total area of the nanoparticles. Next, the confocal fluorescence images were converted to 16-bit grayscale images and imported into ImageJ. The images were processed using the despeckle feature and all pixels of low intensity (2 out of 255 or lower) were ignored to remove noise. The analyze particle feature in ImageJ was used to determine the total area of the fluorescent ATIII on the nanoparticles. The total area was then used to calculate the percent coverage of fluorescent ATIII on the nanoparticles.

Results

Immobilization and functional properties of heparan sulfate bound to magnetic nanoparticles

Biotinylated HS was successfully prepared and immobilized onto streptavidin coated magnetic nanoparticles (Figure 2). The amount of enzyme-accessible HS, determined using heparinase, was 2.7 μg/mg of nanoparticles. This amount reflects the minimum amount biotinylated HS attached to the nanoparticles, which represents only the enzyme-accessible HS.

The activity of 3-OST-1 on HS-linked nanoparticles was determined using [^{35}S]PAPS and scintillation counting. 3-OST-1 (120 μg) catalyzed the transfer of 4 pmol of 3-*O*-sulfo groups to 8.1 μg of HS linked to nanoparticles (Figure 2), which elevated the ^{35}S-radioactivity of the enzymatically modified particles to ~ 70-fold above the control (absence of 3-OST-1 enzyme). This corresponded to the introduction of a ^{35}S — sulfo group onto ~ 5% of the immobilized HS chains. This value is expected based on the specificity of 3-OST-1 for the limited number of modifiable domains present within HS.[14]

After confirming that HS immobilized onto the nanoparticles was capable of being modified by 3-OST-1, we performed modification of immobilized HS on a new set of nanoparticles without using radiolabeling. We then removed the 3-OST-1 from the reaction mixture by precipitating the magnetic nanoparticles and incubated the modified nanoparticles with fluorescent ATIII to investigate the binding properties of the 3-OST-1 modified immobilized HS (Figure 3).

Using confocal microscopy, a pronounced increase in the binding of fluorescent ATIII was observed following 3-OST-1 modification of immobilized HS on nanoparticles (Figure 4 and Supporting Information Figure S2) as compared to unmodified immobilized HS on nanoparticles (Figure 5 and Supporting Information Figure S2). The binding is specific to the modified HS nanoparticles as clearly seen in Figure 4c, the overlay of the fluorescence image (Figure 4a) and the transmitted bright field image (Figure 4b). Analysis using ImageJ software, demonstrated that 32% of the surface area of the 3-OST modified HS nanoparticles bound fluorescent ATIII (Figure 4, d & e and Figure 6), whereas only 0.5% of the surface area of the control unmodified HS nanoparticles bound fluorescent ATIII (Figure 5, d & e and Figure 6).

On-chip modification of heparan sulfate on magnetic nanoparticles and subsequent protein binding assay of modified heparan sulfate

The ability to detect ATIII binding resulting from 3-OST-1 catalyzed modification of HS nanoparticles led us to perform on-chip reactions. Using the digital microfluidic chip, two droplets - one containing 3-OST-1 (40 ng, 1 pmol) and PAPS cofactor (25 μM) and the second containing HS immobilized onto nanoparticles (5.4 ng, 0.4 pmol) - were loaded onto the chip. The chip was then used to drive the droplets to a mixing area by application of an AC voltage of 50 – 100 V_{RMS} to the electrode adjacent to the droplet. The droplets were able to move at a rate of up to 3 electrodes per min, corresponding to about 3 mm per min. Once at the mixing area, the droplets were merged by driving them to the same destination electrode (Figure 7, a-c), followed by homogenizing the reaction droplet by applying voltage (Figure 7, d-f). The reaction droplet was allowed to incubate on the chip for a period of 1 h with an additional homogenizing step at 30 min to keep the nanoparticles in suspension. Following the reaction, we performed a splitting of the reaction droplet to show the potential for additional reactions to be performed in a combinatorial manner (Figure 7, g-i and Supporting Information Figure S2), but then proceeded to rejoin the droplet. The droplets were then recovered from the chip, incubated with fluorescent ATIII, washed to remove excess fluorescent ATIII, and observed using confocal fluorescent microscopy (Figure 8). The results were similar to the experiments performed off-chip (Figure 4) showing a significant increase in the ATIII binding affinity of

the 3-OST-1 modified HS nanoparticles when compared to the unmodified control. Analysis using ImageJ software, demonstrated that 30% of the surface area of the on-chip 3-OST modified HS nanoparticles bound fluorescent ATIII (Figure 6 and Figure 8 d & e), whereas only 0.5% of the surface area of the control unmodified HS nanoparticles bound fluorescent ATIII (Figure 5 d & e and Figure 6). These results confirm that 3-OST-1 can be used to successfully modify nanoparticle immobilized HS in a digital microfluidic system, resulting in HS chains with high ATIII affinity.

Discussion

The loading of HS onto the magnetic nanoparticles was about 20 percent of the manufacturers projected loading capacity, and can be explained by the large steric size of HS. According to manufacturer's specifications, the loading capacity of the streptavidin nanoparticles for the small molecule of biotin-4-fluorescein (MW 645 Da) is 1000 pmol per mg of nanoparticles. We measure a loading of about 200 pmol of HS (average MW 12500 Da) per mg of nanoparticles based on an enzymatic digestion assay.

When the activity of 3-OST-1 on HS-linked nanoparticles was determined by [^{35}S] PAPS and scintillation counting, it was observed that the level of 3-*O*-sulfation was about 70-fold higher on the 3-OST-1 modified nanoparticles compared to the control. Using these values we calculated that 3-OST-1 catalyzed the introduction of a ^{35}S —sulfo group to about 5% of the immobilized HS chains. This value is low because not all HS chains contain an ATIII precursor structure[14] and 3-OST-1 may not have been able to access all of the immobilized HS, e.g., those buried from the surface of the exposed HS chains on the nanoparticles. However, even though the sulfation level was low, there was still an easily measurable increase in HS's binding affinity for ATIII, as detected by confocal microscopy (Figures 4, 5 and 8). Results from the on-chip and off-chip experiments were comparable; 32% of the surface area of the off-chip 3-OST modified HS nanoparticles bound fluorescent ATIII and 30% of the surface area of the on-chip 3-OST modified HS nanoparticles bound fluorescent ATIII (Figure 6). In the images obtained, virtually all the beads from both on-chip and off-chip experiments showed bound fluorescent ATIII (Figures 4 and 8c). As expected, not all of the surface area was covered with fluorescent ATIII, as only 5% of the chains could be modified using 3-OST-1, based on steric factors and the limited number of modifiable domains within HS. The control experiments (Figure 5 and Supporting Information Figure S2) showed virtually no measureable fluorescence associated with non-specific binding. Image analysis demonstrates experimental (specific binding) is ~50-fold greater than control (non-specific binding) (Figure 6).

In summary, this work represents a first step toward the construction of an artificial Golgi organelle through the use of digital microfluidics, recombinant enzyme technology, and magnetic nanoparticles. HS was successfully immobilized onto magnetic nanoparticles and enzymatically modified using 3-OST-1 in a droplet based digital microfluidic device. After enzymatic treatment, the immobilized HS showed high affinity for fluorescent ATIII, confirming its successful modification by 3-OST-1. This represents the first enzymatic modification of an immobilized substrate in a digital microfluidic device and a critical first step in the creation of an artificial Golgi. Work is currently underway to further develop the artificial Golgi into a nano-scale lab-on-a-chip for the synthesis and screening of specific glycans. Such an artificial Golgi will provide a platform for the high throughput synthesis of small amounts of GAGs for biological and pharmacological evaluation. In addition, this tool may be used as a test bed to design biosynthetic heparin, which could replace current unsafe methods of heparin production from animal tissue.[15]

Supplementary Material

Refer to Web version on PubMed Central for supplementary material.

Acknowledgment

The authors acknowledge the National Institutes of Health (HL62244, GM38060, RR023764 to RJL and HL094463 to JL) for supporting this work.

REFERENCES

(1). Twyman, RM. Principles of Proteomics. Garland Science/BIOS Scientific; New York, NY: 2004.

(2). Munoz E, Xu D, Kemp M, Zhang F, Liu J. Biochemistry 2006;45:5122–5128. [PubMed: 16618101]

(3). Esko JD, Selleck SB. Ann. Rev. Biochem 2002;71:435–471. [PubMed: 12045103]

(4). Sasisekharan R, Venkataraman G. Curr. Opin. Chem. Biol 2000;4:626–631. [PubMed: 11102866]

(5). Capila I, Linhardt RJ. Angew. Chem. Int. Ed 2002;41:390–412.

(6). Srinivasan V, Pamula V, Fair R. Lab Chip 2004;4:310–315. [PubMed: 15269796]

(7). Wheeler AR. Science 2008;322:539–540. [PubMed: 18948529]

(8) (a). Srinivasan V, Pamula V, Fair R. Anal. Chim. Acta 2004;507:145–150. (b) Miller EM, Wheeler AR. Anal. Chem 2008;80:1614–1619. [PubMed: 18220413] (c) Moon H, Wheeler AR, Garrell RL, Loo JA, Kim CJ. Lab Chip 2006;6:1213–1219. [PubMed: 16929401] (d) Chang YH, Lee GB, Huang FC, Chen YY, Lin JL. Biomed. Microdevices 2006;8:215–225. [PubMed: 16718406] (e) Barbulovic-Nad I, Yang H, Park P, Wheeler AR. Lab Chip 2008;8:519–526. [PubMed: 18369505]

(9). Wheeler AR. Science 2008;322:539–540. [PubMed: 18948529]

(10). Watson MW, Abdelgawad M, Ye G, Yonson N, Trottier J, Wheeler AR. Anal. Chem 2006;78:7877–7885. [PubMed: 17105183]

(11). Nadkarni VD, Linhardt RJ. Anal. Biochem 1994;222:59–67. [PubMed: 7856872]

(12). Edavettal SC, Lee KA, Negishi M, Linhardt RJ, Liu J, Pedersen LC. J. Biol. Chem 2004;279:25789–25797. [PubMed: 15060080]

(13). Bame KJ, Esko JD. J. Biol. Chem 1989;264:8059–8065. [PubMed: 2524478]

(14). Linhardt RJ, Wang HM, Loganathan D, Bae JH. J. Biol. Chem 1992;267:2380–2387. [PubMed: 1733939]

(15). Guerrini M, et al. Nat. Biotechnol 2008;26:669–675. [PubMed: 18437154]

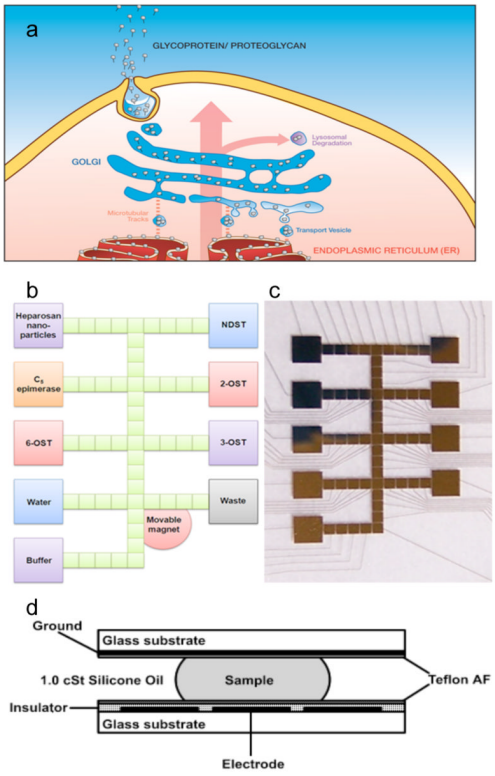

Figure 1.

The Golgi and an artificial Golgi. (a) A cartoon in which the Golgi of a eukaryotic cell is shown in blue. The direction of flow (pink arrow) in posttranslational modification is from the ER (red) to the cell membrane (yellow) where proteoglycans and glycoproteins are released into the extracellular environment. (b) The design of an artificial Golgi for the biosynthesis of HS is shown. Heparosan is modified by a series of biosynthetic enzymes including an *N*-deacetylase/*N*-sulfotransferase (NDST), C_5 epimerase, and 2-, 6-, and 3-*O*-sulfotransferases (2-OST, 6-OST and 3-OST, respectively).[3] Alternatively heparosan can be modified by using a mixture of enzymes to explore the theory of concerted rather then sequential action of the biosynthetic enzymes. The large boxes (multicolor) are reagents and enzyme reservoir electrodes and the small boxes (light green) are electrodes for droplet movement, mixing, and sequestration. (c) A fabricated artificial Golgi based on the design in panel b. The thin lines are gold wires that lead to pads for connection to a power source used to drive the droplets. (d) A diagram showing a cross-section of a droplet sitting over an electrode and overlapping two adjacent electrodes. A glass coverslip on the top of the device contains the ground

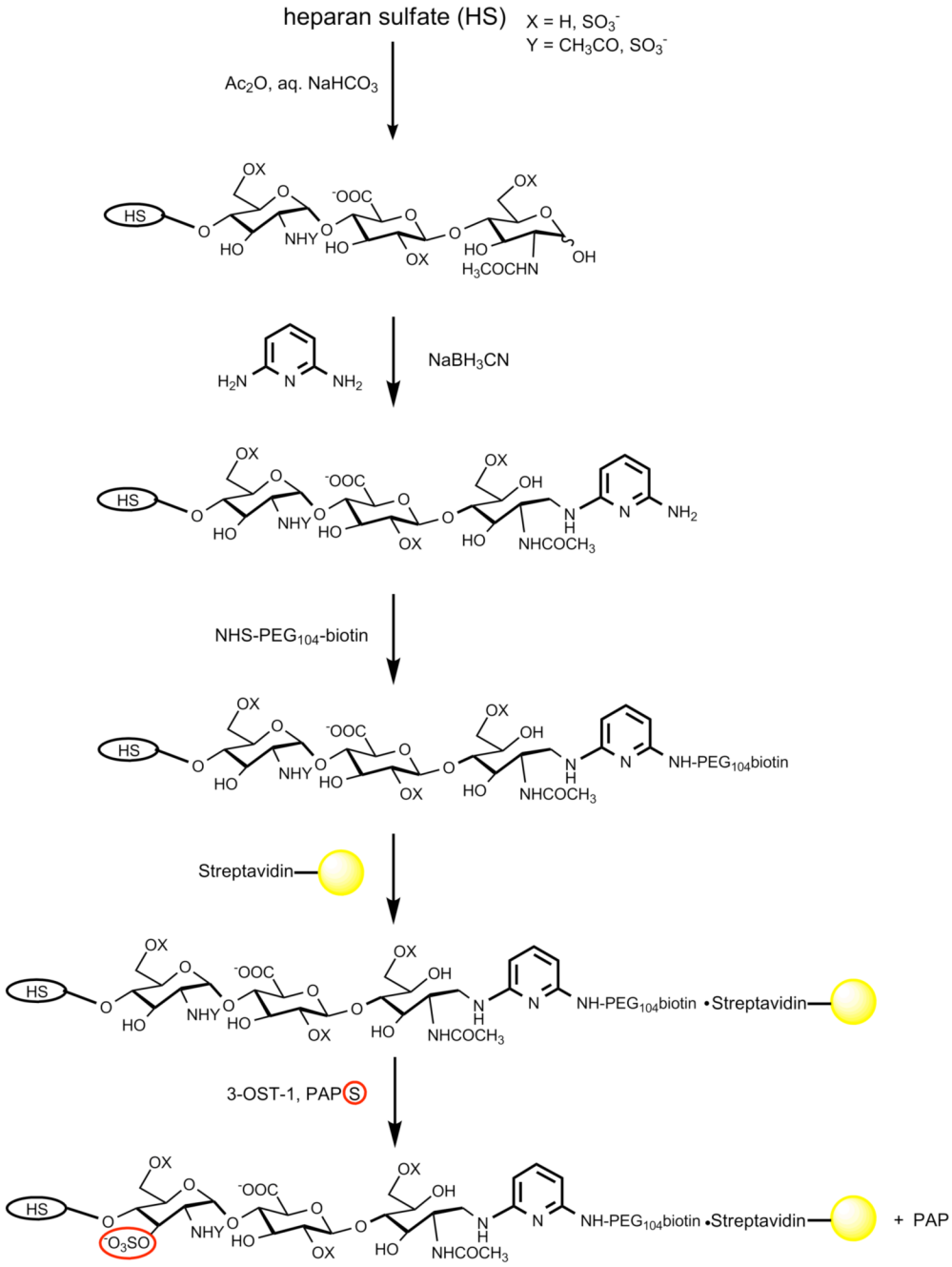

Figure 2.

Chemistry used to immobilize HS substrate onto streptavidin magnetic nanoparticles and subsequent 3-OST-1 modification. Unsubstituted amino groups are first *N*-acetylated and the resulting HS is then reductively aminated with diaminopyridine to which NHS activated PEG_{104}-biotin is attached. The resulting glycoconjungate is then captured by streptavidin magnetic nanoparticles (yellow) and modified by 3-OST-1, which catalyzes the 3-*O*-sulfonation of HS using PAPS cofactor. During this reaction, the sulfo group (red circle) is transferred from the PAPS cofactor to the glucosamine residue on the HS chain. To quantify the level of 3-*O*-sulfonation, [^{35}S]PAPS was used. Scintillation counting measured the transfer of 1 pmol of 3-*O*-sulfo groups to every 2 μg of HS when immobilized to nanoparticles.

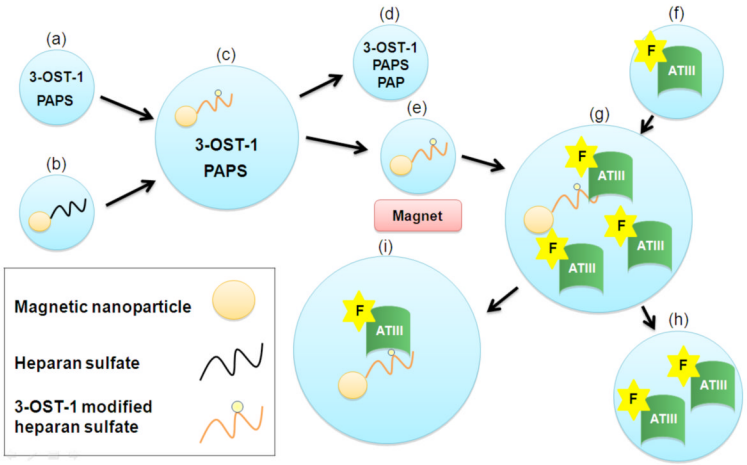

Figure 3.

Schematic of 3-OST-1 modification of immobilized HS on nanoparticles and subsequent detection with fluorescently labeled ATIII taking place on the device shown in Figure 1c. A magnet was used to selectively wash the nanoparticles in solution. The contents of the droplets are labeled as followed (a) 3-OST-1 enzyme with PAPS (b) immobilized HS (c) Modification of HS by 3-OST-1 (d) Removal of 3-OST-1, excess PAPS, and PAP (e) Modified HS (f) Fluorescently labeled ATIII (g) Mixing of fluorescent ATIII with modified immobilized HS (h) Excess fluorescently labeled ATIII removed from washing step (i) Fluorescence detection of modified HS on nanoparticles.

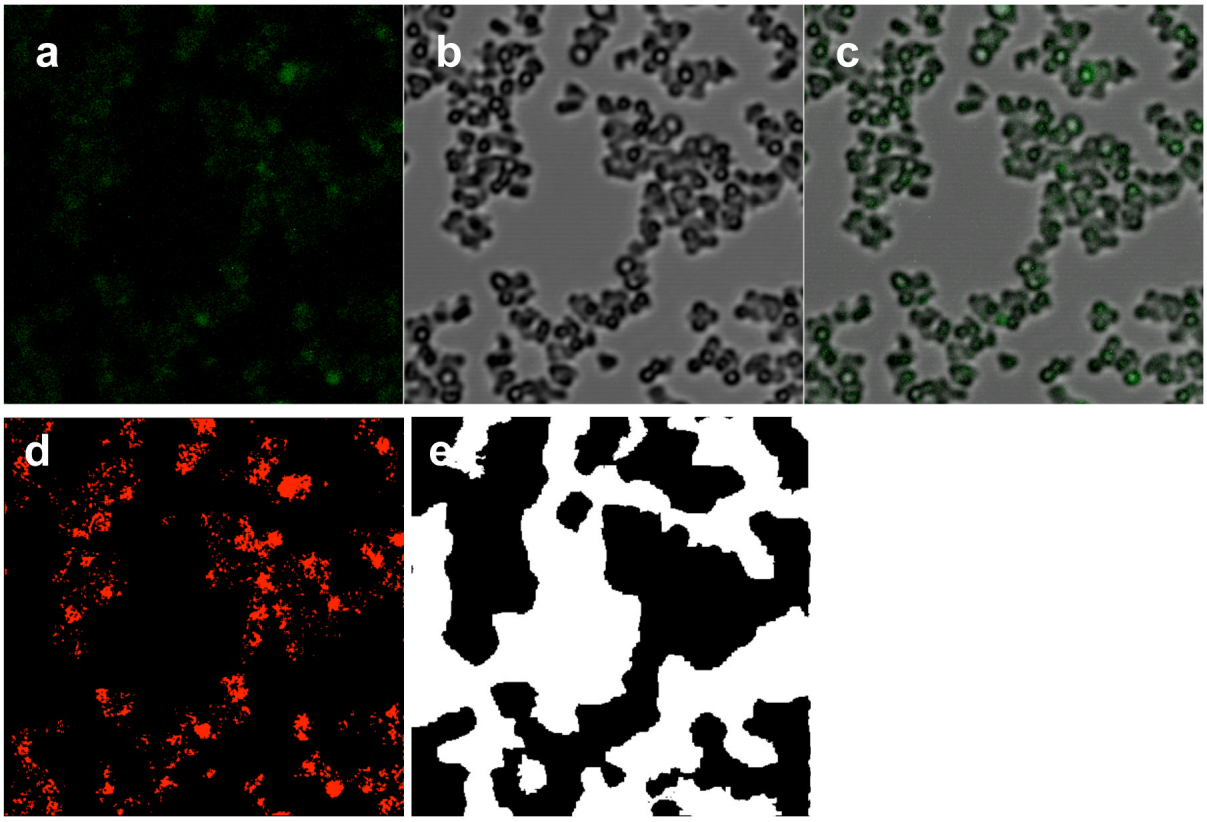

Figure 4.
Confocal images and image analysis of HS nanoparticles modified off-chip with 3-OST-1 and probed with fluorescent ATIII and washed. (a) Fluorescence image of ATIII bound to 3-OST-1 modified HS nanoparticles. (b) Transmitted bright field image of 3-OST-1 modified HS nanoparticles (c) Overlay of (a) and (b). (d) Fluorescence area selected by ImageJ from (a) shown in red. (e) Nanoparticle area selected by ImageJ from (b).

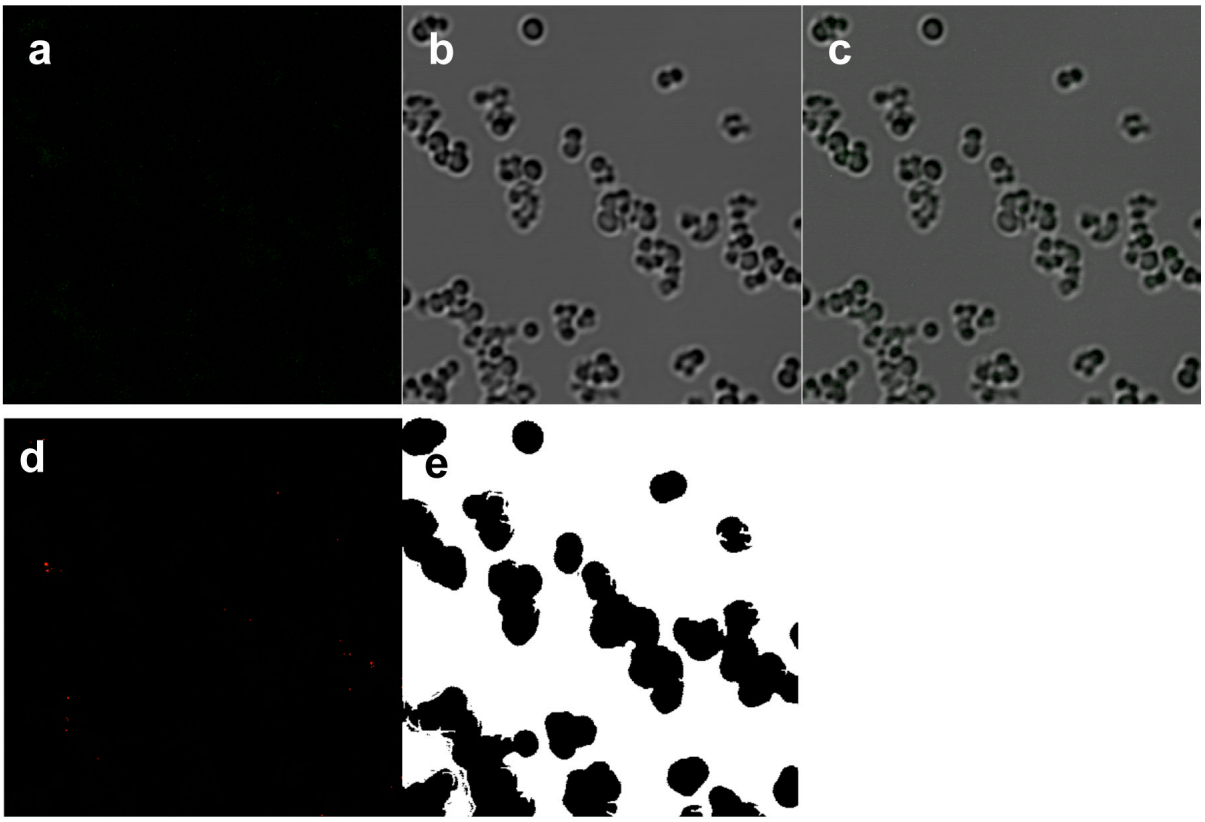

Figure 5.
Confocal images and image analysis of control unmodified HS nanoparticles probed with fluorescent ATIII and washed. (a) Fluorescence image of ATIII bound to 3-OST-1 modified HS nanoparticles. (b) Transmitted bright field image of 3-OST-1 modified HS nanoparticles (c) Overlay of (a) and (b). (d) Fluorescence area selected by ImageJ from (a) shown in red. (e) Nanoparticle area selected by ImageJ from (b).

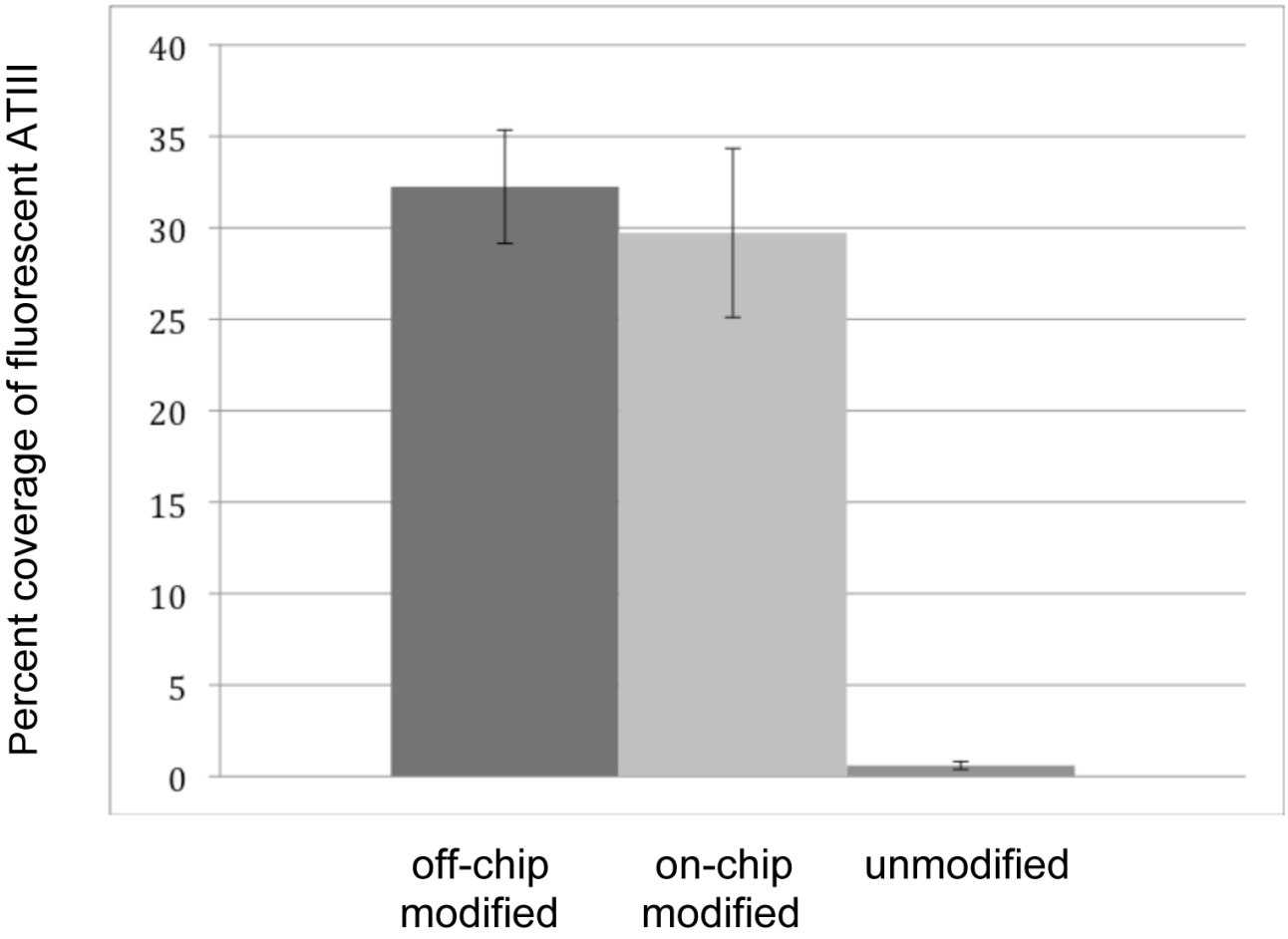

Figure 6.
Graph comparing the percent coverage of fluorescent ATIII on unmodified HS nanoparticles, 3-OST-1 off-chip modified HS nanoparticles, and 3-OST-1 on-chip modified HS nanoparticles. Both the off-chip and on-chip 3-OST-1 modified HS nanoparticles show a significant increase in ATIII binding affinity when compared to the unmodified control. Error bars are standard deviations based on n = 4.

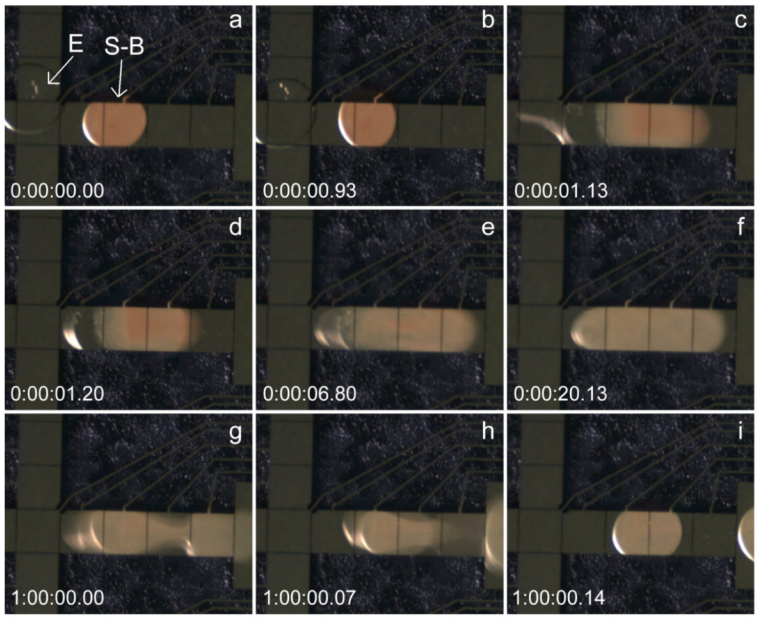

Figure 7.

Video sequence of on-chip enzymatic modification of immobilized HS on nanoparticles by 3-OST-1 enzyme. Time stamps in h:min:sec format. (a-c) Small circular droplet containing 3-OST-1 enzyme and PAPS in PBS buffer (E) is joined with a small circular droplet containing HS substrate immobilized on magnetic nanoparticles (S-B) in 1.13 s. (d-f) Large oval droplet containing reaction components are mixed by stretching. (g-i) Large oval droplet can be split into equal sized smaller circular droplets with one taken off chip for analysis and the other used in secondary reactions.

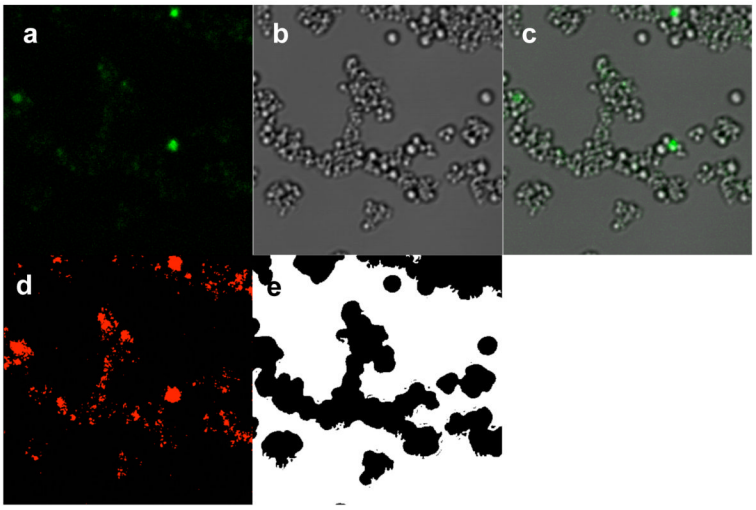

Figure 8.
Confocal images and image analysis of HS nanoparticles modified on-chip with 3-OST and probed with fluorescent ATIII and washed. (a) Fluorescence image of ATIII bound to 3-OST-1 modified HS nanoparticles. (b) Transmitted bright field image of 3-OST-1 modified HS nanoparticles (c) Overlay of (a) and (b). (d) Fluorescence area selected by ImageJ from (a) shown in red. (e) Nanoparticle area selected by ImageJ from (b).